06

Synthesis and research of carbon and palladium-based composites

© G.N. Churilov,[1,2] V.G. Isakova,[1] V.I. Elesina,[1,2] N.G. Vnukova,[1,2] N.S. Nikolaev,[1] E.V. Tomashevich,[1,3] G.A. Glushenko,[1] V.A. Lopatin[1]

[1]Kirensky Institute of Physics, FSBSI Federal Research Center „Krasnoyarsk Science Center SB RAS“,
660036 Krasnoyarsk, Russia
[2]Siberian Federal University, Institute of Engineering Physics and Radio Electronics,
660074 Krasnoyarsk, Russia
[3]Institute of Chemistry and Chemical Technology of the Siberian Branch of the Russian Academy of Sciences, FSBSI Federal Research Center „Krasnoyarsk Science Center SB RAS“,
660036 Krasnoyarsk, Russia
e-mail: churilov@iph.krasn.ru

Received November 1, 2024
Revised November 1, 2024
Accepted November 1, 2024

In the present work, we report the synthesis of nanosized palladium/carbon powder in an alternating current arc discharge plasma (66 kHz) and the production of composite materials based on it through thermal oxidation in a flow of argon containing 20 wt.% oxygen. Using methods such as transmission electron microscopy, X-ray photoelectron spectroscopy, X-ray phase analysis, X-ray fluorescence analysis, powder X-ray diffraction, differential thermal analysis, and Raman scattering, we conducted the identification of substances in the samples. We also investigated the morphology, elemental, structural and phase composition, chemical and electronic state of atoms on the surface of the obtained samples, as well as the stoichiometric and structural changes that occurred during the thermal oxidation process. The results of cyclic voltammetry studies of ethanol oxidation reactions in alkaline electrolyte on graphite electrodes coated with composite palladium/carbon powders were presented, allowing for a comparison of their electrochemical behaviour depending on the composition of the composite. The behaviour of the samples in the electrochemical oxidation reaction of ethanol in an alkaline electrolyte was recorded by monitoring the current changes in the peak potential region during the experiment. In particular, it was shown that a multiple increase in the peak current value was demonstrated by a sample containing a mixture of Pd/PdO_2.

Keywords: nanoparticles, composite palladium/carbon materials, thermal oxidation, electrochemical properties, electrode materials.

DOI: 10.61011/TP.2025.02.60839.370-24

Introduction

In high-tech industries, composite materials consisting of two or more components replace traditional materials. Composite materials have a set of advantages associated with a combination of miscellaneous structural components in a single material offering wide opportunities for varying the properties of such materials through the rational selection of components and component ratios and distribution, dispersion, morphology, etc. [1].

Recent literature data analysis demonstrates wide use of composite materials in various industries and technologies, they rank first among innovative engineering materials [2–7].

Due to their considerable physical capabilities, carbon-based composite materials have promising future in various practical applications [8]. It is known that carbon may be used to produce materials featuring high specific surface area, various pore sizes and high electron conductivity [9,10]. Carbon in the allotropic modification of graphite and in the form of glass carbon is widely used as a carrier of substances accelerating electrochemical reactions, in various sensors and other power industry applications [11–19]. Significant focus is also made on the study of palladium-based and palladium-carbon-based materials primarily in the form of graphite, i.e. sp^2-hybridization [20–23]. Palladium plays an important role in most industrial applications due to its unique properties, it has a well-pronounced structure, and outstanding physical and thermal stability. Transition metal nanoparticles (including palladium) demonstrate high catalytic activity [24,25], high thermal stability [26], thus, making them suitable for repeated use [27,28].

Nanomaterials with Pd are used in catalyst production [29–31]. There are studies investigating oxidation-reduction processes with fullerenes and palladium applied to them [32,33] which show that such powders also have high catalytic activity.

Particles containing palladium oxides attract special attention due to their interesting properties in terms of applicability [34–36]. Oxygen-containing groups on carbon dots play an important role in Pd(II) reduction to Pd(0), nanoparticle growth control [35].

In [37], a method is proposed for producing electroactive palladium-based materials by means of AC (66 kHz) electrochemical palladium dispersion. A set of more probable chemical and electrochemical processes flowing in AC conditions is discussed. Electrochemical activity of

Pd−PdO/C materials in ethanol alkaline oxidation reaction is defined by the presence of oxide phase and palladium particle size — it is maximum for materials with minor prevalence of palladium oxides.

Production of composite materials is needed in order to take advantage of each type of material and minimize their disadvantages. Composite materials with desired properties may be achieved by various methods. Chemical and other methods for nanoscale particle preparation are known [15,38–41]. For example, a method for preparing a composite material consisting of a carbon matrix and metallic component, whose content is 35%, is described in [42].

Study [43] reports about the fabrication of carbon-based Pd clusters from metal wire electrodes by a solution plasma spray technique. The obtained Pd/C nanoclusters demonstrated a good electrochemical activity, their long-term electrochemical stability was examined.

A profound experimental experience shows that the use of traditional plasma techniques and commercial frequency DC or AC arc discharge generators is not adequately efficient and easily controllable. This study intends to develop plasma-chemical techniques for producing powder nano-composite materials in low-frequency arc discharge plasma on the basis of carbon, palladium and palladium oxides that are capable of accelerating electrochemical reactions.

1. Samples and research methods

Nanocomposite material properties depend considerably not only on the chemical composition, but also on the powder particle shape, size and other factors. This is explained by the interest of researchers in the problem of producing powders with minimum particle sizes. This problem may be solved using plasma-chemical synthesis. In particular, for the purpose of this work, synthesis was carried out in arc discharge plasma using a nanomaterial synthesis system [44].

Selection of a nanoparticle carrier with chemical reaction accelerating activity is critical because the carrier plays an important role in stabilization of an active reaction-accelerating phase. For carbon-palladium-based nanopowder synthesis, graphite (sp^2-hybridization of carbon) was chosen as the most suitable material for noble metal nanoparticle synthesis [28,45]. Emission spectral analysis graphite rods 6 mm in diameter and 100 mm in length (TC 3497-001-51046676-2008) were used as electrodes. Holes 3.5 mm in diameter and 85 mm in length were drilled in the rods and filled with metallic palladium powder mixed with graphite powder. The amount of palladium was 28 wt.%. Palladium and graphite rods were annealed at 0.27 kPa and 1400°C. Annealed palladium and graphite rods were sprayed in arc discharge in helium at 130 kPa. Arc discharge parameters were as follows: current 240 A, arc frequency 66 kHz. As a result, carbon and palladium powder, called the carbon condensate, was prepared and contained palladium in nanodisperse state (PCC) and hereinafter referred to as sample 1.

Changes taking place in sample 1 during heating were examined in an open crucible 5 cm in height in argon also containing 20 wt.% oxygen, flow rate — 2 l/min. The crucible bottom was heated to 1000°C, and the temperature of the top of crucible was 700°C (this is the temperature range that includes the palladium oxide decomposition temperature — 830°C). Heating was maintained during 20 min, as a result sample 1 was visually divided into two parts with almost equal volume that were collected into different containers and examined. Lower part of the powder was black, a typical color for carbon materials, (sample 2), and the upper part was light-gray (sample 3).

Structures of the samples were studied by powder X-ray diffraction. Spectra were recorded using the DRON-4-07 diffractometer in monochromatized Cu-Kα radiation in 0.001° steps and with exposition 5 s.

Structural and morphological examinations of the samples were performed by the transmission electron microscopy (TEM) using the Hitachi TEM HT7700 microscope.

Energy spectra were recorded by X-ray photoelectron spectroscopy (XPS) using the UNI-SPECS (SPECS) photoelectron spectrometer with PHOIBOS-150-MCD-9 hemispherical analyzer and FOCUS-500 X-ray monochromator (AlKαradiation, $h\nu = 486.74$ eV). High-resolution spectra were recorded at an analyzer transmission energy of 10 eV. Surface contamination was removed by Ar^+ 1 kV ions. Binding energy scale was preliminary calibrated by Au 4f 7/2 (84.00 eV) and Cu2p3/2 (932.63 eV) positions. Aliphatic carbon line with the binding energy of 285 eV was used for binding energy correction. Spectra were processed in CasaXPS.

Differential thermal analysis (DTA) was performed using the NETZSCH STA 449C thermal analyzer with QMS 403C mass-spectrometer in argon containing 20 wt.% oxygen.

Elemental composition of the samples was measured by the X-ray fluorescence analysis using the Hitachi SEM S-5500 scanning electron microscope.

Raman scattering spectroscopy (RSS) analysis was performed using the Horiba Jobin Yvon T64000 Raman-scattering spectrometer.

Cyclic voltammograms (CVA) were recorded using a circuit containing of an electrochemical cell with three electrodes (main electrode, platinum counter electrode and Ag/AgCl reference electrode) submersed into electrolyte solution and connected to the PI-50-Pro „Elins“ potentiostat-galvanostat.

As main electrodes, the initial graphite electrode was coated by drop application of „ink“ prepared by ultrasonic mixing of samples 1−3 and Nafion (Liquiontm Solution LQ-115 1100EW, 15 wt.%, Ion Power, GmbH) polymer solution in water, hereinafter the electrodes were designated as: electrodes E1, E2 and E3. CVA were prepared in 0.1M KOH + 0.1M C_2H_5OH solution in air in the

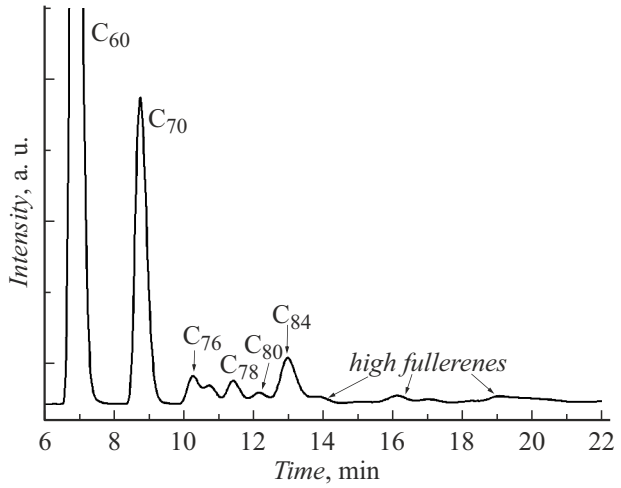

Figure 1. Chromatogram of a soluble portion extracted from sample 1.

potential range from −100 to 1200 mV at a scanning rate of 100 mV/s.

The fullerene mixture was extracted from PCC using our proprietary procedure and a system described in [46,47]. Composition of the fullerene mixture included in PCC was evaluated using the Agilent 1200 liquid chromatograph with the Cosmosil Buckyprep (4.6 × 250 mm) column. Toluene was used as the eluent, exposure time was 40 min, eluent flow rate was 5 ml/min. Relative content of various types of extracted fullerenes was evaluated by ratio of a peak area, corresponding to an individual fullerene, to the total area of all peaks in the chromatogram.

Sample 1 turned out to contain a soluble fraction that was 10.4 wt.% of the extracted portion of sample 1 after extraction and re-dissolution. Chromatogram is shown in Figure 1. It can be seen that the sample is a fullerene mixture that is usually formed even without palladium introduction [44].

The procedure as described above was used to establish the following fullerene mixture composition (rel.%): C_{60} — 57.13; C_{70} — 29.72; C_{76} — 3.01; C_{78} — 1.92; C_{80} — 1.66; C_{84} — 2.99; higher fullerenes — 3.57.

2. Findings and discussion

X-ray fluorescence analysis identified the elemental composition of sample 1 (C — 79.7; Pd — 18.4; balance — 1.9 wt.%).

Figure 2 shows the X-ray diffraction pattern of sample 1. X-ray diffraction analysis established that all reflexes corresponded to the lattice of palladium (2Θ 39.45°; 46.16°; 67.29°; 82.08°; 86.08°) and graphite (26.27°).

Figure 3, *a* shows the microscopic image of sample 1 recorded by the TEM method. It was found that sample 1 consisted of rounded palladium particles 4 nm to 20 nm in diameter distributed in carbon (Pd/C).

DTA analysis of sample 1 is shown in Figure 3, *b*. DTA identified typical endothermic and exothermic reactions taking place in the test sample. Gas release in the mass-spectrometer was observed at three temperatures: at 210°C — organic impurity were burned (simultaneous release of $H_2O + CO_2$); at 515°C — CO_2 was released, which corresponded to exothermic effected with loss of weight. Endothermic effect with loss of weight (oxygen release during expected decomposition of palladium oxide at 820−831°C) didn't appear in the mass spectrum against the background of high oxygen concentration in the mixture. As a result of such heating, the weight of sample decreased by 54.8 wt.% as early as at 750°C. The loss of weight is caused by the oxidation of amorphous carbon, graphite and fullerene. Then, at 830°C, endothermic reaction with loss of weight is observed. This effect is well known and associated with palladium reduction [48].

The order and layout of thermal effects (i.e. upward or downward deviation of the curve) on the DTA indicate that transformation of the studied substance was moderate, but quite fast, because the line of the major peak, that can be seen at 450°C, is asymmetric and decreases sharply and, thus, quite rapidly already at ≈ 500°C.

XPS spectra analysis showed that metallic Pd and PdO_2 [49,50] were present in samples 1 and 3 (Figure 4, *a, b*, respectively). Carbon binding energy corresponds to sp^2-hybridization and carbon as part of functional groups with C−O and C=O bonds (Figure 5, *a, b*, respectively) [51]. Line C1s spectrum of samples 1 and 3 shows that carbon is mainly in sp^2-hybridization, C−O and C=O functional groups are also present. Sample 3 contains a small amount of palladium (less than 1%).

X-ray fluorescence analysis identified the elemental composition of sample 2 (C — 91.1; Pd — 7.7; balance — 1.2 wt.%) and of sample 3 (C — 1.1; Pd — 95.7; balance — 3.2 wt.%). As can be seen, sample 3 has a sponge-like texture (Figure 6, *b*), i.e. the substance has a large developed surface compared with sample 2 (Figure 6, *a*).

Figure 7 shows electron microscope images of sample 3 obtained by the TEM method with different scale

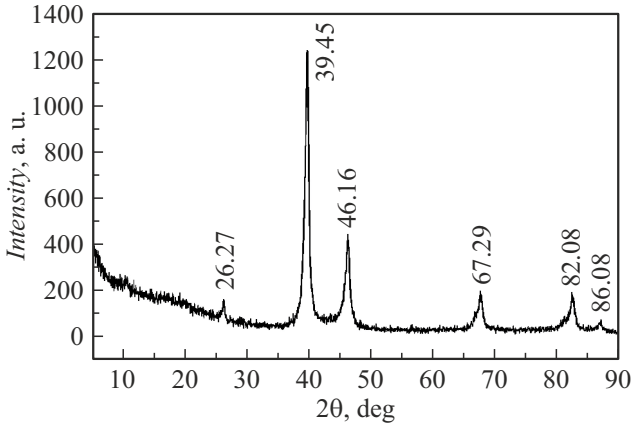

Figure 2. X-ray pattern for sample 1. Cu-Kαradiation.

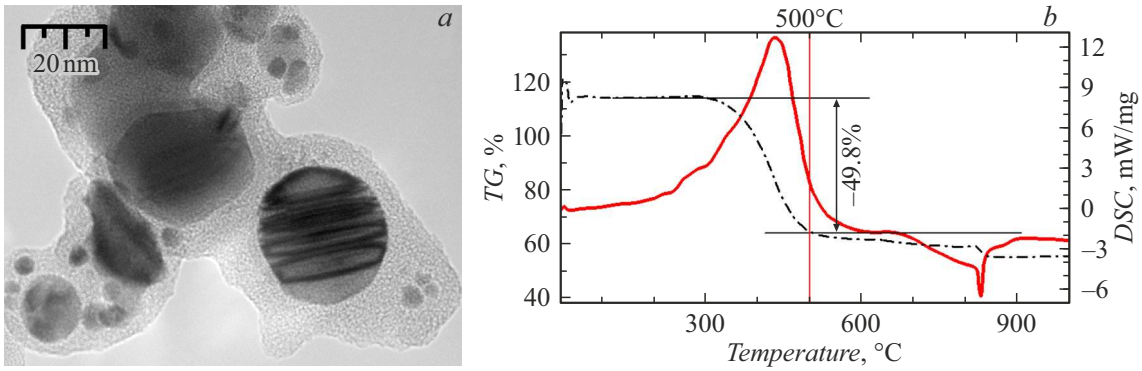

Figure 3. Sample 1: *a* — microscopic image; *b* — thermogram.

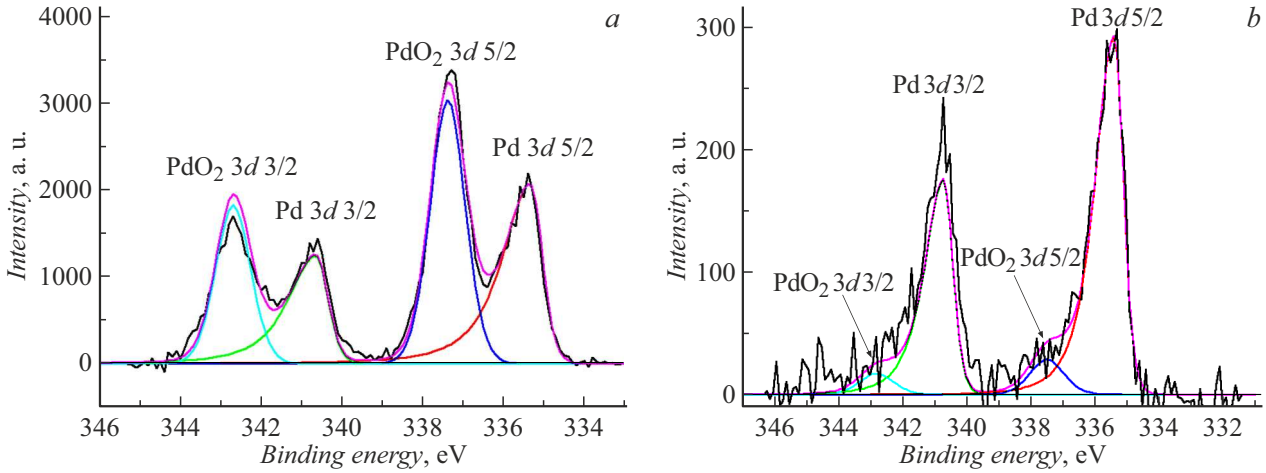

Figure 4. XPS spectrum of Pd3d line: *a* — sample *1*, *b* — sample *3*.

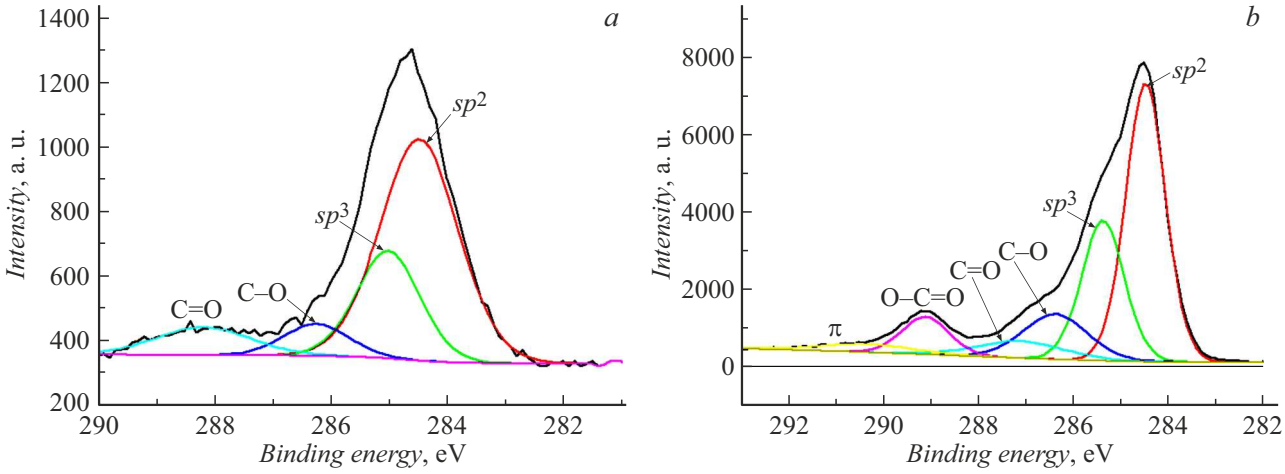

Figure 5. XPS spectrum of C1s line: *a* — sample *1*, *b* — sample *3*.

of magnification. Figure 7, *a* shows dense palladium particles with a mean size of 30 ± 10 nm. Figure 7, *b* shows high resolution electron microscope image containing nanoparticles with a mean size of 15 ± 5 nm. Atomic interplanar spacings observed in Figure 7, *b* are equal to 0.45 nm, which corresponds to d(100) phase of PdO_2 (space group $P4_2/mnm$, lattice parameters: $a = b = 0.4483$ nm; $c = 0.3101$ nm).

Analysis of diffraction reflexes observed in the electron diffraction pattern of sample 3 (Figure 8) shows that

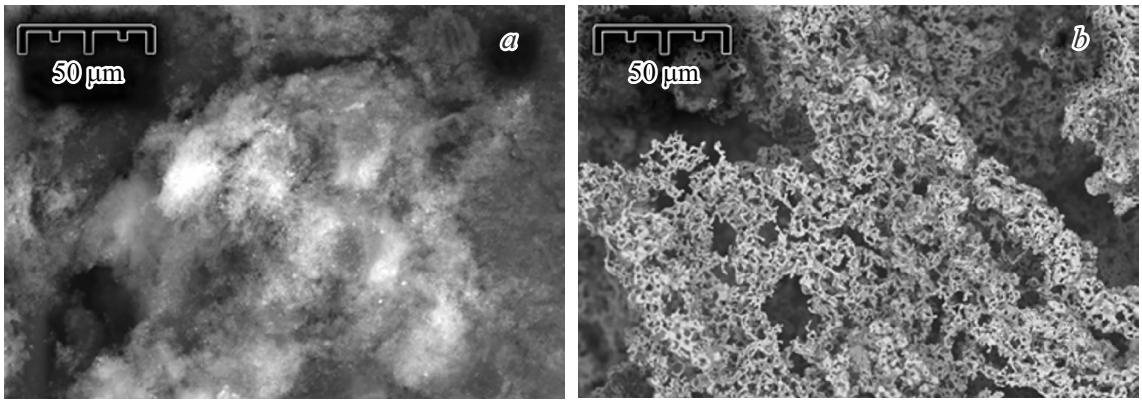

Figure 6. SEM image: *a* — sample 2, *b* — sample 3.

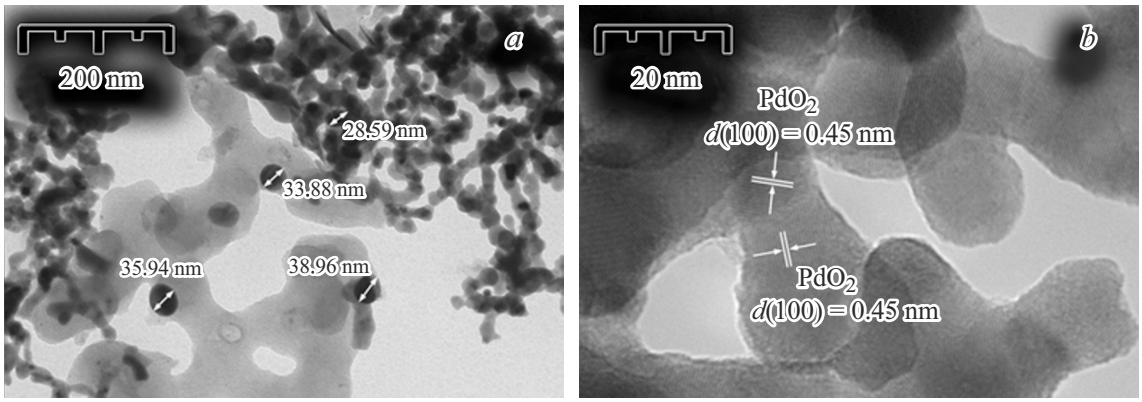

Figure 7. Electron microscope images of sample 3: *a* — scale 200 nm, *b* — scale 20 nm.

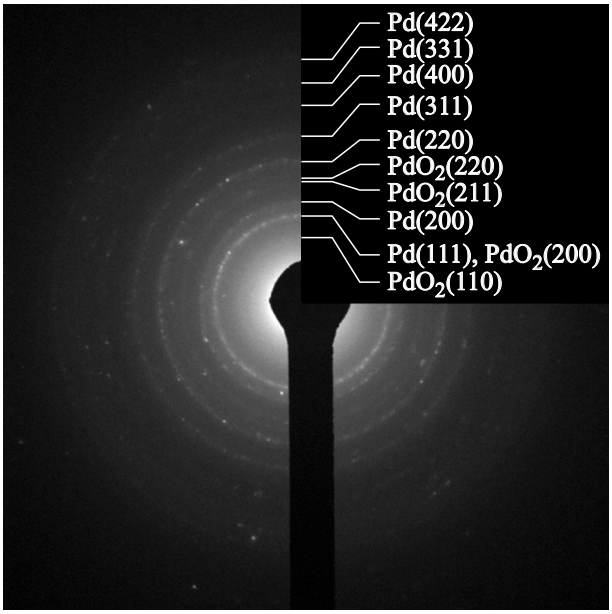

Figure 8. Electron diffraction pattern of sample 3.

palladium with the face-centered cubic lattice (space group Fm-3m, lattice parameter: $a = 0.389$ nm) is the main phase in the sample. There are also diffraction reflexes that have low intensity and correspond to PdO_2 phase (space group $P4_2/mnm$, lattice parameters: $a = b = 0.4483$ nm; $c = 0.3101$ nm).

RS spectroscopy analysis identified carbon and palladium oxide in sample 3. Figure 9, *a, b* shows the RS analysis of samples 2 and 3, respectively.

RS spectrum (Figure 9) of sample 2 has bands *D* and *G* of nanodispersive carbon, disordered and ordered forms of carbon, respectively, and a low-intensity peak that is assigned to oxidized palladium [52]. RS spectrum of sample 3 has an intense peak corresponding to molecular vibrations of palladium oxide. Results obtained by the RS method confirmed that carbon and palladium oxide were present in sample 2 (carbon with minor palladium oxide impurities) and sample 3 (carbon with considerable content of palladium oxide).

Figure 10 shows ethanol oxidation CVA on electrodes E1 (Figure 10, *a*), E2 (Figure 10, *b*), E3 (Figure 10, *c*). The dashed line in Figure 10, *a* shows CVA for the initial graphite electrode, and it can be seen that it has no any peak currents.

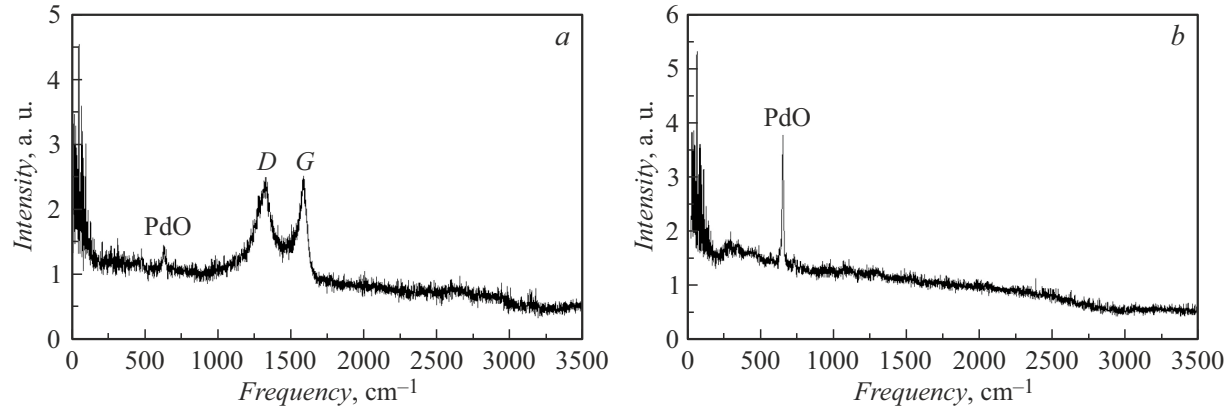

Figure 9. RS spectra: *a* — sample 2, *b* — sample 3.

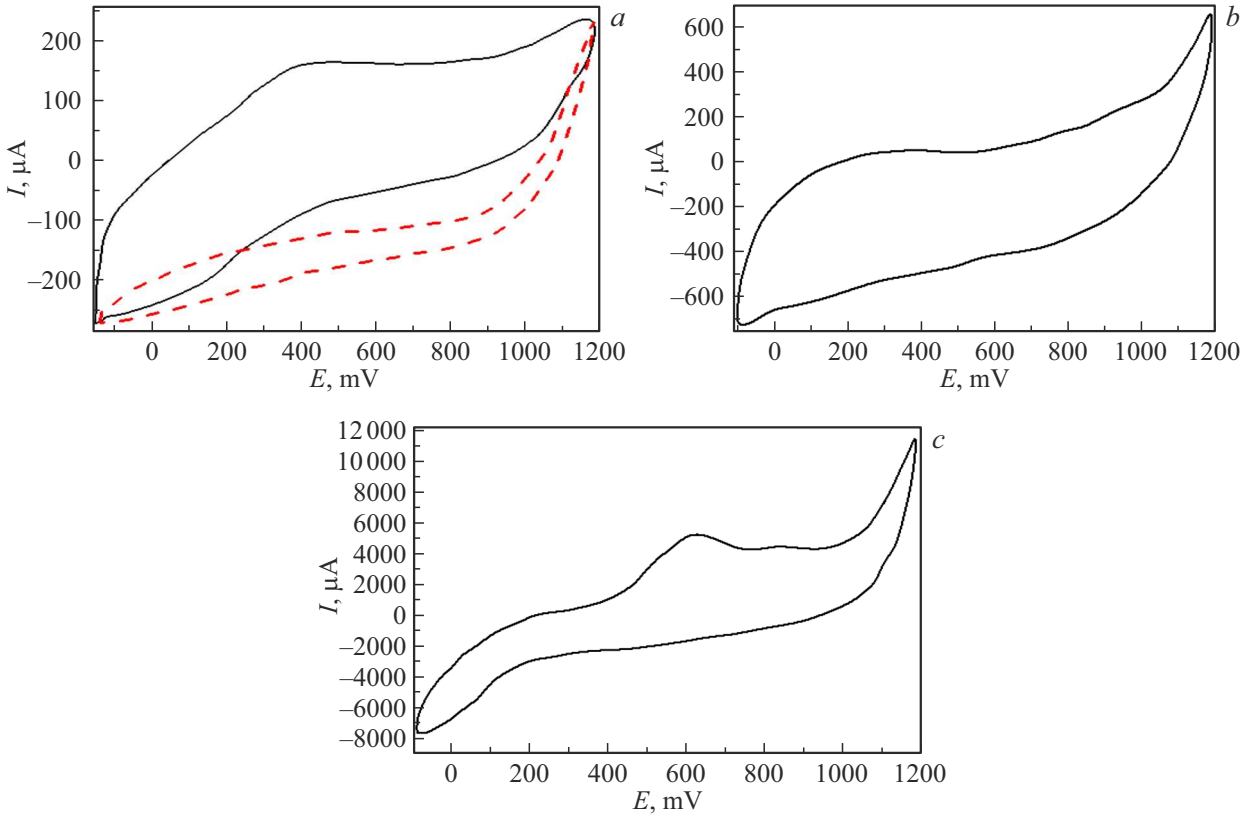

Figure 10. Ethanol oxidation CVA in 0.1M KOH + 0.1M C_2H_5OH mixture on electrodes: *a* — E1; *b* — E2; *c* — E3, potential scan rate — 100 V/s. Dashed line corresponds to CVA of the initial graphite electrode.

In the voltammograms of ethanol oxidation on electrodes E1 and E2, a region from -100 to ~ 100 mV in anode and cathode potential scanning is assigned to hydrogen sorption/desorption. It is known that palladium nanoparticles are able to sorb hydrogen atoms in their bulk structure at low potentials [53]. In CVA of sample E3, this is a region from -100 to ~ 200 mV, which corresponds to higher activity in hydrogen oxidation reduction [54].

With anode scanning, potential ~ 400 mV with peak current 120 μA on electrode E1 corresponds to ethanol oxidation. On electrode E2, potential at 200 mV, but with the minimum peak current, corresponds to alcohol oxidation. On electrode E3, ethanol oxidation takes place at 630 mV with current peak $\sim 5000\,\mu$A, which exceeds considerably the readings on electrodes E1 and E2.

Conclusion

According to the study, the fitted parameters of kHz arc discharge plasma made it possible to synthesize a

composite nanomaterial in the form of powder with palladium particles distributed in carbon particles with various hybridization (graphite, fullerenes). Palladium particle sizes were from 4 nm to 20 nm.

According to the X-ray fluorescence analysis, the composite nanomaterial (sample 1) contained: C — 79.7; Pd — 18.4; balance — 1.9 wt.%. After nanomaterial treatment (sample 1) by thermal oxidation in argon containing 20 wt.% oxygen in the gradient temperature field, visual separation of the nanomaterial into two parts was observed. The lower part was black and contained: C — 91.1; Pd — 7.7; balance — 1.2 wt.% (sample 2), and the upper part was gray and contained: C — 1.1; Pd — 95.7; balance — 3.2 wt.% (sample 3).

Cyclic voltammetry of the behavior of obtained composite nanomaterials in electrochemical oxidation reaction of ethanol in alkaline electrolyte showed that high electrochemical activity of sample 1 was caused by the presence of fullerene (10.4 wt.%),and in sample 3 — by the high concentration of metallic palladium and palladium oxide mixture. Sample 2, where the palladium content in the carbon composite material was 7.7 wt.%, had low activity in the electrochemical oxidation reaction of ethanol compared with samples 1 and 3.

Multiple increase in peak current corresponding to ethanol oxidation on electrode containing sample 3 (5000 μA, 630 mV) compared with readings on the electrode containing sample 1 (120 μA, 200 mV) is indicative of much higher activity in the ethanol oxidation reaction of sample 3 that contained palladium and palladium oxides (Pd/PdO_2). Thus, composite nanomaterials (samples 1 and 3) may be successfully used for the development of electrode materials.

Acknowledgments

The authors would like to express appreciation to the Shared Research Facility „Federal Research Center„ Krasnoyarsk Science Center, Siberian Branch of Russian Academy of Sciences“, for the equipment provided for this study.

The authors are particularly grateful to A.V. Cherepakhin, S.N. Vereshchagin, M.N. Volochaev, A.M. Zhizhaev, A.S. Krylov and S.M. Zharkov for analytical research and assistance in interpreting the obtained results.

Funding

The study was performed within the research theme of the state assignment of Kirensky Institute of Physics.

Conflict of interest

The authors declare no conflict of interest.

References

[1] L. Huang, L. Geng, H. Peng. Progr. Mater. Sci., **71** (10), 93 (2015). DOI: 10.1016/j.pmatsci.2015.01.002
[2] G. Balaganesan, V.C. Khan. Compos B Eng., **98**, 39 (2016). DOI: 10.1016/j.compositesb.2016.04.083
[3] S. Guinard, O. Allix, D. Gué dra-Degeorges, A. Vinet. Compos. Sci. Technol., **62** (4), 585 (2002). DOI: 10.1016/S0266-3538(01)00153-1
[4] N.M. Nurazzi, M.R.M. Asyraf, S.F. Athiyah, S.S. Shazleen, S.A. Rafiqah, M.M. Harussani, S.H. Kamarudin, M.R. Razman, M. Rahmah, E.S. Zainudin, R.A. Ilyas, H.A. Aisyah, M.N.F. Norrrahim, N. Abdullah, S.M. Sapuan, A. Khalina. Polymers, **13**, 2170 (2021). DOI: 10.3390/polym13132170
[5] R. Yahaya, S.M. Sapuan, M. Jawaid, Z. Leman, E.S. Zainudin. Def. Technol., **12** (1), 52 (2016). DOI: 10.1016/j.dt.2015.08.005
[6] H. Han, H. Sun, F. Lei, J. Huang, S. Lyu, B. Wu, M. Yang, C. Zhang, D. Li, Z. Zhang, D. Sun. ES Mater. Manuf., **15**, 53 (2021). DOI: 10.30919/esmm5f523
[7] B. Zhao, L. Liang, Z. Bai, X. Guo, R. Zhang, Q. Jiang, Z. Guo. ES Energy Environ, **14**, 79 (2021). DOI: 10.30919/esee8c488
[8] M.M. Harussani, S.M. Sapuan, G. Nadeem, T. Rafin, W. Kirubaanand. Defence Technol., **18** (8), 1281 (2022). DOI: 10.1016/j.dt.2022.03.006
[9] S.M. Manocha. Sadhana, **28**, 335 (2003). DOI: 10.1007/BF02717142
[10] E. Pérez-Mayoral, I. Matos, M. Bernardo, I.M. Fonseca. Catalysts, **9** (2), 133 (2019). DOI: 10.3390/catal9020133
[11] E. Lam, J.H.T. Luong. ACS Catal., **4** (10), 3393 (2014). DOI: 10.1021/cs5008393
[12] J.C. Ndamanisha, L.-P. Guo. Analyt. Chim. Acta., **747**, 19 (2012). DOI: 10.1016/j.aca.2012.08.032
[13] J. Zhang, M. Terrones, C.R. Park, R. Mukherjee, M. Monthioux, N. Koratkar, Y.S. Kim, R. Hurt, E. Frackowiak, T. Enoki, Y. Chen, Y. Chen, A. Bianco. Carbon, **98**, 708 (2016). DOI: 10.1016/j.carbon.2015.11.060
[14] P. Veerakumar, K.-C. Lin. Chemosphere, **253**, 126750 (2020). DOI: 10.1016/j.chemosphere.2020.126750
[15] Y.-H. Chen, W.-F. Luo, J.-A. Chen, J. Wang. Chin. J. Chem. Phys., **32**, 218 (2019). DOI: 10.1063/1674-0068/cjcp1812301
[16] A. Cabiac, T. Cacciaguerra, P. Trens, R. Durand, G. Delahay, A. Medevielle, D. Plée, B. Coq. Appl. Catalysis A: General, **340** (2), 229 (2008). DOI: 10.1016/j.apcata.2008.02.018
[17] M. Rabchinskii, V.V. Sysoev, O.E. Glukhova, M. Brzhezinskaya, D.Yu. Stolyarova, A.S. Varezhnikov, M.A. Solomatin, P.V. Barkov, D.A. Kirilenko, S.I. Pavlov, M.V. Baidakova, V. Shnitov, N.S. Struchkov, D.Yu. Nefedov, A. Antonenko, P. Cai, Z. Liu, P. Brunkov. Adv. Mater. Technol., **7** (7), 2101250 (2022). DOI: 10.1002/admt.202101250
[18] M.K. Rabchinskii, V.V. Sysoev, A.S. Varezhnikov, M.A. Solomatin, N.S. Struchkov, D.Yu. Stolyarova, S.A. Ryzhkov, G.A. Antonov, V.S. Gabrelian, P.D. Cherviakova, M.V. Baidakova, A.O. Krasnova, M. Brzhezinskaya, S.I. Pavlov, D.A. Kirilenko, V.A. Kislenko, S.V. Pavlov, S.A. Kislenko, P.N. Brunkov. ACS Appl. Mater. Interfaces, **15** (23), 28370 (2023). DOI: 10.1021/acsami.3c02833
[19] W. Dong, S. Cheng, C. Feng, N. Shang, S. Gao, C. Wang. Catalysis Commun., **90**, 70 (2017). DOI: 10.1016/j.catcom.2016.11.021

[20] M. Lüsi, H. Erikson, M. Merisalu, M. Rähn, V. Sammelselg, K. Tammeveski. J. Electroanalyt. Chem., **834**, 223 (2019). DOI: 10.1016/j.jelechem.2018.12.061
[21] D.P. Chen, X.C. Liu, X. Liu, L. Yuan, M.L. Zhong, C.Y. Wang. Intern. J. Hydrogen Energy, **46** (59), 30455 (2021). DOI: 10.1016/j.ijhydene.2021.06.167
[22] A.M. Sheikh, E.L. Silva, L. Moares, L.M. Antonini, M.Y. Abellah, C.F. Malfatti. American J. Mining Metallurgy, **2** (4), 64 (2014). DOI: 10.12691/ajmm-2-4-1
[23] O.A. Hjortshøj Schreyer, J. Quinson, M. Escudero-Escribano. Inorganics, **8** (11), 59 (2020). DOI: 10.3390/inorganics8110059
[24] B. Chen, D. Chao, E. Liu, M. Jaroniec, N. Zhao, S.-Z. Qiao. Energy Environ. Sci., **13**, 1096 (2020). DOI: 10.1039/c9ee03549d
[25] W. Chen, W. Wu, Z. Pan, X. Wu, H. Zhang. J. Alloys Compd., **763**, 257 (2018). DOI: 10.1016/j.jallcom.2018.05.301
[26] M. Najem, A.A. Nada, M. Weber, S. Sayegh, A. Razzouk, C. Salameh, C. Eid, M. Bechelany. Materials, **13** (8), 1947 (2020). DOI: 10.3390/ma13081947
[27] O.A. Cano, C.A.R. González, J.F.H. Paz, P.A. Madrid, P.E.G. Casillas, A.L.M. Hernández, C.A.M. Pérez. Catal. Today, **282** (2), 168 (2017). DOI: 10.1016/j.cattod.2016.06.053
[28] L. Minati, K.F. Aguey-Zinsou, V. Micheli, G. Speranza. Dalton Transactions, **47** (41), 14573 (2018). DOI: 10.1039/C8DT02839G
[29] A. Chen, C. Ostrom. Chem. Rev., **115** (21), 11999 (2015). DOI: 10.1021/acs.chemrev.5b00324
[30] A.J.M. Mackus, M.J. Weber, N.F.W. Thissen, D. Garcia-Alonso, R.H.J. Vervuurt, S. Assali, A.A. Bol, M.A. Verheijen, W.M.M. Kessels. Nanotechnology, **27** (3), 034001 (2016). DOI: 10.1088/0957-4484/27/3/034001
[31] C.H. Moon, N.V. Myung, E.D. Haberer. Appl. Phys. Lett., **105**, 223102 (2014). DOI: 10.1063/1.4903245
[32] Z. Bai, L. Niu, S. Chao, H. Yan, Q. Cui, L. Yang, J. Qiao, K. Jiang. Int. J. Electrochem. Sci., **8** (7), 10068 (2013). DOI: 10.1016/S1452-3981(23)13032-X
[33] X. Yang, M. Zhen, G. Li, X. Liu, X. Wang, C. Shu, L. Jiang, C. Wang. J. Mater. Chem. A, **28** (1), 8105 (2013). DOI: 10.1039/C3TA11907F
[34] C. Wang, F. Yang, W. Yang, L. Ren, Y. Zhang, X. Jia, L. Zhang, Y. Li. RSC Adv., **35** (5), 27526 (2015). DOI: 10.1039/C4RA16792A
[35] W. Zhao, T. Wang, B. Wang, R. Wang, Y. Xia, M. Liu, L. Tian. Colloids Surf. A: Physicochem. Eng. Aspects, **658**, 130677 (2023). DOI: 10.1016/j.colsurfa.2022.130677
[36] C.J. Crawford, Y. Qiao, Y. Liu, D. Huang, W. Yan, P.H. Seeberger, S. Oscarson, S. Chen. Organic Process Research & Development, **25** (7), 1573 (2021). DOI: 10.1021/acs.oprd.0c00536
[37] N.A. Faddeev, A.B. Kuriganova, I.N. Leontyev, N.V. Smirnova. Dokl. RAN, Khimiya, nauki o materialakh, **507** (1), 59 (2022).(in Russian) DOI: 10.31857/S2686953522600441
[38] O.E. Gudko, N.V. Smirnova, T.A. Lastovina, V.E. Guterman. Nanotechnol. Russ., **4** (5-6), 309 (2009). DOI: 10.1134/S1995078009050085
[39] W. Zhai, L. Bai, R. Zhou, X. Fan, G. Kang, Y. Liu, K. Zhou. Adv. Sci., **8** (11), 2003739 (2021). DOI: 10.1002/advs.202003739
[40] H.H.P. Yiu, I.J. Bruce, F. McGuinness, P.A. Wright. In: *Studies in Surface Science and Catalysis*, ed. by S.-E. Park, R. Ryoo, W.-S. Ahn, C.W. Lee, J.-S. Chang (Elsevier, 2003), p. 146, 57. DOI: 10.1016/S0167-2991(03)80326-9
[41] A.A. Khouya, H. Ba, W. Baaziz, J.-M. Nhut, A. Rossin, S. Zafeiratos, O. Ersen, G. Giambastiani, V. Ritleng, C. Pham-Huu. ACS Appl. Nano Mater., **4** (2), 2265 (2021). DOI: 10.1021/acsanm.1c00002
[42] E. Tsushima, N. Suzuki. (Patent EP 1 055 650, 2000) https://patentimages.storage.googleapis.com/61/60/97/a6f46b78d43eb3/EP1055650A1.pdf
[43] J. Shi, X. Hu, J. Zhang, W. Tang, H. Li, X. Shen, N. Saito. Progr. Natural Sci.: Mater. Intern., **24** (6), 593 (2014). DOI: 10.1016/j.pnsc.2014.10.011
[44] G.N. Churilov, W. Krätschmer, I.V. Osipova, G.A. Glushenko, N.G. Vnukova, A.L. Kolonenko, A.I. Dudnik. Carbon, **62**, 389 (2013). DOI: 10.1016/j.carbon.2013.06.022
[45] M.J. Weber, A.J. Mackus, M.A. Verheijen, C. van der Marel, W.M. Kessels. Chem. Mater., **24** (15), 2973 (2012). DOI: 10.1021/cm301206e
[46] V.I. Elesina, G.N. Churilov, N.G. Vnukova, N.S. Nikolaev, G.A. Glushenko, V.G. Isakova. Fullerenes, Nanotubes and Carbon Nanostructures, **30** (5), 553 (2022). DOI: 10.1080/1536383X.2021.1966421
[47] G.N. Churilov, V.I. Elesina. *Ustroistvo dlya razdeleniya veshchestva na rastvorimuyu i nerastvorimuyu tchasti* (Patent RU 2744434, 2021), (in Russian) https://findpatent.ru/patent/274/2744434.html
[48] P.K. Gallagher, M.E. Gros. J. Thermal Analysis, **31**, 1231 (1986). DOI: 10.1007/bf01914636
[49] B. Lesiak, B. Mierzwa, P. Jiricek, I. Bieloshapka, K. Juchniewicz, A. Borodzinski. Appl. Surf. Sci., **458**, 855 (2018). DOI: 10.1016/j.apsusc.2018.07.137
[50] L.S. Kibis, A.I. Titkov, A.I. Stadnichenko, S.V. Koscheev, A.I. Boronin. Appl. Surf. Sci., **255**, 9248 (2009). DOI: 10.1016/j.apsusc.2009.07.011
[51] M. Brzhezinskaya, I.V. Mishakov, Y.I. Bauman, Y.V. Shubin, T. A. Maksimova, V.O. Stoyanovskii, E.Yu. Gerasimov, A.A. Vedyagin. Appl. Surf. Sci., **590**, 153055 (2022). DOI: 10.1016/j.apsusc.2022.153055
[52] T. Kumari, R. Gopal, A. Goyal, J. Joshi. J. Inorganic and Organometallic Polymers and Mater., **29**, 316 (2019). DOI: 10.1007/s10904-018-1001-x
[53] M. Schwarzer, N. Hertl, F. Nitz, D. Borodin, J. Fingerhut, T.N. Kitsopoulos, A.M. Wodtke. J. Phys. Chem. C, **126** (34), 14500 (2022). DOI: 10.1021/acs.jpcc.2c04567
[54] F. Chekin. Bull. Mater. Sci., **38** (4), 887 (2015). DOI: 10.1007/s12034-015-0954-4

Translated by E.Ilinskaya